Orientation dependence of the critical magnetic field for multiferroic BiFeO$_3$

Randy S. Fishman

Materials Science and Technology Division, Oak Ridge National Laboratory, Oak Ridge, Tennessee 37831, USA

Multiferroic BiFeO$_3$ undergoes a transition from a distorted spiral phase to a G-type antiferromagnet above a critical field H_c that depends on the field orientation **m**. We show that $H_c(\mathbf{m})$ has a maximum when oriented along a cubic diagonal parallel to the electric polarization **P** and a minimum in the equatorial plane normal to **P** when two magnetic domains with the highest critical fields are degenerate. The orientational dependence of $H_c(\mathbf{m})$ is more complex than indicated by earlier work, which did not consider the competition between magnetic domains. Some recent measurements might be explained by a mixture of magnetic domains.

PACS number(s): 75.30.Kz, 75.50.Ee

I. INTRODUCTION

Multiferroic materials offer the tantalizing prospect of controlling magnetic properties with an electric field and electric properties with a magnetic field. Because of their technological promise, multiferroic materials remain the subject of intense interest. Of all known multiferroic materials, only BiFeO$_3$ exhibits multiferroicity at room temperature. As a type-I or "proper" multiferroic, BiFeO$_3$ has a ferroelectric transition temperature[1] $T_c \approx 1100$ K significantly higher than its Néel transition temperature[2] $T_N \approx 640$ K. Although the ferroelectric polarization is only slightly enhanced[3–5] by the formation of a distorted spin cycloid, the magnetic domain distribution of BiFeO$_3$ can be manipulated with an applied electric field.[6,7]

The unwinding of the cycloid with magnetic field as it transforms into an antiferromagnet provides insight about the nature of the interactions that produce the multiferroic behavior in BiFeO$_3$ and about the competition between magnetic domains. This paper evaluates the critical magnetic field $H_c(\mathbf{m})$, above which the cycloid for a particular domain is destroyed, as a function of the field orientation **m**.

Using single crystals of BiFeO$_3$ that have recently become available, inelastic neutron-scattering measurements[8–10] of the spin-wave spectra determined the nearest and next-nearest antiferromagnetic (AF) exchange interactions $J_1 \approx -4.5$ meV and $J_2 \approx -0.2$ meV on the psuedocubic unit cell with lattice constant[11] $a = 3.96$ Å sketched in Fig. 1. Because the wavelength $\lambda \approx 62$ nm of the cycloid is so long,[2,6,12–14] however, inelastic neutron-scattering measurements[9,15] are unable to resolve excitations about the magnetic satellites $(2\pi/a)(0.5 \pm \delta, 0.5 \mp \delta, 0.5)$ $(\delta = a/(\sqrt{2}\lambda) \approx 0.0045)$, on either side of the antiferromagnetic (AF) Bragg wave vector $\mathbf{Q}_0 = (\pi/a)(1,1,1)$. Consequently, inelastic neutron scattering cannot determine the very small interaction energies of less than 1 meV that control the cycloid.

By contrast, the spin-wave modes at the ordering wave vectors **Q** of the cycloid can be measured very precisely with Raman[16] or THz spectroscopy.[17,18] The excellent agreement[18,19] between the observed and predicted THz modes confirms that a microscopic model[20] with easy-axis anisotropy $K \approx 0.0035$ meV along the electric polarization direction $\mathbf{z}' = (1,1,1)$ (all unit vectors are assumed normalized to 1) and two Dzalyoshinskii-Moriya (DM) interactions can describe the

multiferroic behavior of BiFeO$_3$. Whereas the DM interaction $D \approx 0.107$ meV normal to the cycloidal plane fixes the cycloidal wavelength, the DM interaction[21–24] $D' \approx 0.054$ meV along $\mathbf{z}' = (1,1,1)$ produces a small cycloidal tilt[23] that alternates in sign from one $[1,1,1]$ hexagonal plane to the next.

If the DM and anisotropy interactions were absent, then J_1 and J_2 would stabilize a G-type AF with ferromagnetic (FM) order within each $[1,1,1]$ hexagonal plane. The distorted cycloid can be destabilized in favor of this antiferromagnet by chemical impurities,[25] strain,[26] and magnetic[3–5] or electric fields.[27] In the AF phase, the DM interaction D' produces a weak FM moment[4,5,28] M_0 between 0.03 and 0.06 μ_B per $S = 5/2$ Fe^{3+} ion due to the canting of the moments within each hexagonal plane.

With the electric polarization $\mathbf{P} = P\mathbf{z}'$ along any of the eight equivalent cubic diagonals, the three magnetic domains of BiFeO$_3$ have wave vectors $\mathbf{Q}_n = \mathbf{Q}_0 + \mathbf{q}_n$ where $\mathbf{q}_1 = (2\pi/a)(\delta, -\delta, 0)$, $\mathbf{q}_2 = (2\pi/a)(\delta, 0 - \delta)$, and $\mathbf{q}_3 = (2\pi/a)(0, \delta, -\delta)$. For domain n, we construct a coordinate system with $\mathbf{x}'_n$ along $\mathbf{q}_n$ and $\mathbf{y}'_n = \mathbf{z}' \times \mathbf{x}'_n$. For $\mathbf{z}' = (1,1,1)$, the coordinate axis for each magnetic domain is given in Fig. 1. In the zero field, the three domains of bulk BiFeO$_3$ are degenerate and equally occupied.

In a magnetic field, however, the degeneracy of the domains may be lifted. Generally, the domain with the lowest energy in a magnetic field $\mathbf{H} = H\mathbf{m}$ has the largest value of $|\mathbf{y}'_n \cdot \mathbf{m}|$, so that the spins of that domain lie predominantly perpendicular to the field. For a hemisphere of **m** with polarization **P** along $\mathbf{z}' = (1,1,1)$, the solid curves in Fig. 2 denote the boundaries between the domains with the lowest energies and the highest critical fields. Domains 1, 2, and 3 are degenerate when $\mathbf{m} = \pm\mathbf{z}'$. For $\mathbf{m} = (0,0,1)$, domain 1 has the lowest energy and domains 2 and 3 remain degenerate with higher energies.[19] THz measurements[18] indicate that domains 2 and 3 are then depopulated above about 6 T. Those measurements also indicate that it may be possible to reduce the population of the metastable domains by first applying a field far above H_c and then reducing it to $H < 6$ T.

The microscopic model used to solve for the critical fields is presented in Sec. II. Section III provides results for the critical fields $H_c^{(n)}(\mathbf{m})$ of each domain (both stable and metastable) and Sec. IV compares those results with measurements. A short conclusion is provided in Sec. V.
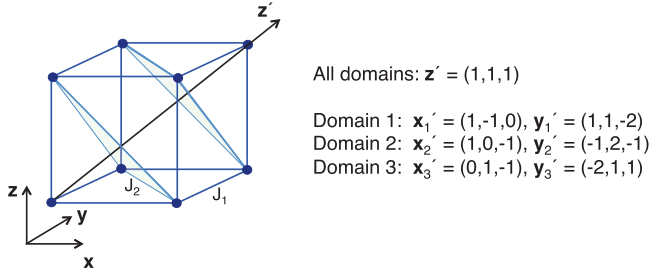
FIG. 1. (Color online) The exchange interactions J_1 and J_2 on the pseudocubic lattice for $BiFeO_3$ with Fe^{3+} ions at the corners and the notation for the three magnetic domains with electric polarization along $\mathbf{z}' = (1,1,1)$.

II. MICROSCOPIC MODEL

The Hamiltonian for spins in domain n is given by

$$
\mathcal{H} = -J_1 \sum_{\langle i,j \rangle} \mathbf{S}_i \cdot \mathbf{S}_j - J_2 \sum_{\langle i,j \rangle'} \mathbf{S}_i \cdot \mathbf{S}_j
$$

$$
- D_1 \sum_{\mathbf{R}_j = \mathbf{R}_i + \sqrt{2}a\mathbf{u}_n^{\pm}} \mathbf{y}_n' \cdot (\mathbf{S}_i \times \mathbf{S}_j)
$$

$$
- D_2 \sum_{\mathbf{R}_j = \mathbf{R}_i + \sqrt{2}a\mathbf{x}_n'} \mathbf{y}_n' \cdot (\mathbf{S}_i \times \mathbf{S}_j)
$$

$$
- D' \sum_{\mathbf{R}_j = \mathbf{R}_i + a\mathbf{x}, a\mathbf{y}, a\mathbf{z}} (-1)^{R_{iz'}/c} \mathbf{z}' \cdot (\mathbf{S}_i \times \mathbf{S}_j)
$$

$$
- K \sum_i (\mathbf{S}_i \cdot \mathbf{z}')^2 - 2\mu_B H \sum_i \mathbf{S}_i \cdot \mathbf{m}, \tag{1}
$$

where $\mathbf{u}_n^{\pm} = \mathbf{x}_n'/2 \pm \sqrt{3}\mathbf{y}_n'/2$. Among the nearest neighbors in the hexagonal plane normal to $\mathbf{z}'$, D_1 couples $\mathbf{R}_i$ to $\mathbf{R}_i + \sqrt{2}a\mathbf{u}_n^{\pm}$ and D_2 couples $\mathbf{R}_i$ to $\mathbf{R}_i + \sqrt{2}a\mathbf{x}_n'$.

To the order of $\vartheta(\delta^2) < 10^{-4}$, the same static and dynamic properties are produced by any values for D_1 and D_2 with the sum $D = D_1 + D_2$. As found earlier,[15] $D \approx 0.107$ meV produces the observed period $\lambda = a/\sqrt{2}\delta \approx 62$ nm in zero field. For $\mathbf{m} = (0,0,1)$, changing $D_1 = 0$ to $D_2 = 0$ but keeping $D_1 + D_2 = 0.107$ meV shifts the critical field by about 0.01%. In previous work,[15,19,20] we followed the convention of Ref. 8 by taking $D_2 = 0.107$ meV and setting $D_1 = 0$. Without D', the Hamiltonian of Eq. (1) was first proposed by Sosnowska and Zvezdin.[29]

For each domain, the inverse DM mechanism[30–32] induces the cycloidal polarization

$$
\mathbf{P}^{\text{ind}} = \lambda_1 \sum_{\mathbf{R}_j = \mathbf{R}_i + \sqrt{2}a\mathbf{u}_n^{\pm}} \mathbf{u}_n^{\pm} \times (\mathbf{S}_i \times \mathbf{S}_j)
$$

$$
+ \lambda_2 \sum_{\mathbf{R}_j = \mathbf{R}_i + \sqrt{2}a\mathbf{x}_n'} \mathbf{x}_n' \times (\mathbf{S}_i \times \mathbf{S}_j), \tag{2}
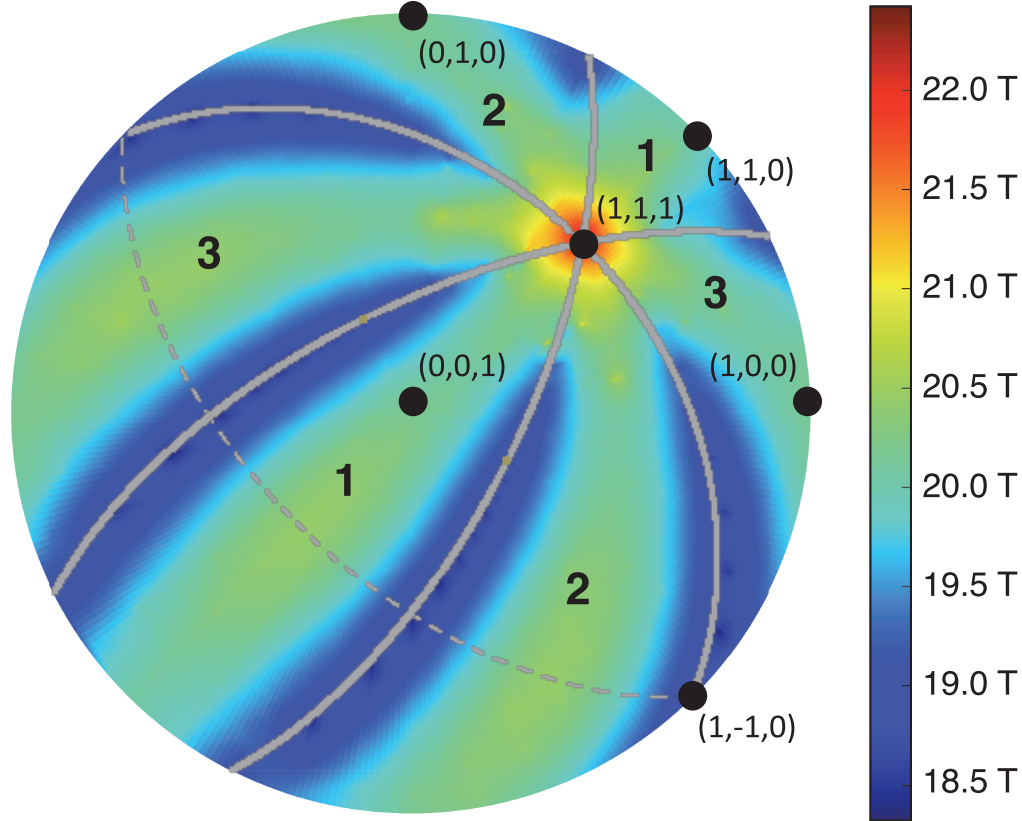$$

FIG. 2. (Color) The variation of H_c over a hemisphere of $\mathbf{m}$, with a maximum along the polarization direction $\mathbf{z}' = (1,1,1)$. Gray lines are the borders between magnetic domains (denoted by 1, 2, or 3) with the highest H_c. The dashed line is the equator when the north pole coincides with $\mathbf{z}'$.

which is parallel to $\mathbf{z}' = (1,1,1)$. In analogy with the results for the D_1 and D_2 terms in the Hamiltonian, the induced polarization $P^{\mathrm{ind}} \approx 4\pi S^2 \lambda_c \delta$ along $\mathbf{z}'$ only depends on the sum $\lambda_c = \lambda_1/2 + \lambda_2$. Compared to the ferroelectric polarization[33] $P \approx 100\ \mu\mathrm{C/cm}^2$ above T_{N} or H_c, the induced polarization[4,5] $P^{\mathrm{ind}} \approx 40\ \mathrm{nC/cm}^2$ below T_{N} or H_c is quite small. Using this value for P^{ind} gives $\lambda_c \approx 113\ \mathrm{nC/cm}^2$ or 4.38×10^{-11} e cm/site.

With the same spin state in hexagonal layers m and $m+2$, layers $m = 1$ and 2 are parameterized as

$$S_{x'}(\mathbf{R}) = A^{(m)}(\mathbf{R}) \sin \mu \cos \tau^{(m)} \sin \left(2\pi \delta R_{x'}/a + \gamma_1^{(m)} \right) + s_0 p_{x'}^{(m)}, \tag{3}$$

$$S_{y'}(\mathbf{R}) = A^{(m)}(\mathbf{R}) \sin \mu \sin \tau^{(m)} \sin \left(2\pi \delta R_{x'}/a + \gamma_2^{(m)} \right) + s_0 p_{y'}^{(m)}, \tag{4}$$

$$S_{z'}(\mathbf{R}) = A^{(m)}(\mathbf{R}) \cos \mu F^{(m)}(\mathbf{R}) + s_0 p_{z'}^{(m)}, \tag{5}$$

where

$$F^{(m)}(\mathbf{R}) = \sum_{l=1} C_{2l-1} \cos[2(2l-1)\pi \delta R_{x'}/a] + \sum_{l=1} C_{2l} \cos(4l\pi \delta R_{x'}/a + \Gamma^{(m)}), \tag{6}$$

and we take $C_1 = 1$. The unit vectors $\mathbf{p}^{(m)}$, tilt angles $\tau^{(m)}$, phases $\gamma_1^{(m)}$, $\gamma_2^{(m)}$, and $\Gamma^{(m)}$ can be different for layers 1 and 2. In a magnetic field, $F^{(m)}(\mathbf{R})$ contains both even and odd harmonics C_l, which may be out of phase due to $\Gamma^{(m)}$. On layer m and site $\mathbf{R}$, the amplitude $A^{(m)}(\mathbf{R})$ is fixed by the condition that $|\mathbf{S}(\mathbf{R})| = S$, which is satisfied by a quadratic equation for $A^{(m)}(\mathbf{R})$. The lower root is used for layer 1; the upper root is used for layer 2.

Because C_l falls off rapidly with l, we neglect harmonics above $l = 4$. Fixing $\delta = 1/p$, where $p \gg 1$ is an integer, the energy $E = \langle \mathcal{H} \rangle$ is minimized over the 17 variational parameters $(\mu, \tau^{(m)}, \gamma_i^{(m)}, \Gamma^{(m)}, \mathbf{p}^{(m)}, C_{l \leqslant 4},$ and $s_0)$ on a unit cell with p sites along $\mathbf{x}'_n$ and two hexagonal layers. An additional minimization loop over p determines the cycloidal wave vector as a function of field. In zero field, $p = 222$ and $\lambda = ap/\sqrt{2} \approx 62$ nm. Although they do not diverge at the first-order transition between the cycloidal and AF phases, λ and p increase by roughly a factor of two between $H = 0$ and H_c.

III. CRITICAL FIELD

We use Eq. (1) to evaluate the critical magnetic field H_c as a function of its orientation $\mathbf{m}$. Beginning with the variational parameters known for zero field, H is increased in increments of about 0.015 T until the AF phase achieves a lower energy than the cycloidal phase, at which point the energies of both phases are interpolated to solve for $H_c(\mathbf{m})$. This time-consuming procedure is required by the large number of variational parameters that determine the spin state in Eqs. (3)–(5).

Results for the critical field as a function of $\mathbf{m}$ are given by the contours of Fig. 2 over a hemisphere of $\mathbf{m}$ with $\mathbf{z} = (0,0,1)$ at the top. In agreement with Ref. 34, $H_c(\mathbf{m})$ depend only

on the angles $\zeta = \cos^{-1}(\mathbf{m} \cdot \mathbf{z}')$ and $\psi = \cos^{-1}(\mathbf{m} \cdot \mathbf{x}'_1)$ of the magnetic field with respect to the electric polarization. While H_c achieves a maximum when $\mathbf{m}$ lies along $\mathbf{z}'$ ($\zeta = 0$), it is a minimum in the equatorial plane normal to $\mathbf{z}'$ ($\zeta = \pi/2$) when the two magnetic domains with the highest critical fields are degenerate. We find that $H_c(\mathbf{m})$ varies by about 4 T, from a minimum of 18.4 T to a maximum of 22.4 T. Since $H_c(\mathbf{m}) = H_c(-\mathbf{m})$, the results of Fig. 2 can also be used to obtain $H_c(\mathbf{m})$ around $(0,0,-1)$ with another maximum at $-\mathbf{z}'$.

By contrast, Tokunaga *et al.*[4] argued that $H_c(\mathbf{m})$ is a function only of ζ and is independent of ψ. Assuming a purely harmonic and coplanar cycloid, Le Bras *et al.*[34] obtained a simple expression for the dependence of $H_c(\mathbf{m})$ on both ζ and ψ. However, they did not consider the competition between cycloids in different magnetic domains. Due to the complexity of our model, we are unable to directly compare our numerical results for $H_c(\mathbf{m})$ with the analytic expression of Ref. 34 for a given domain.

The competition between magnetic domains produces the complex dependence of $H_c(\mathbf{m})$ on ζ and ψ. Along the dashed equator ($\zeta = \pi/2$) sketched in Fig. 2, the critical fields $H_c^{(n)}(\mathbf{m})$ for each domain are separately plotted versus ψ in Fig. 3. While the individual critical fields $H_c^{(n)}(\mathbf{m})$ vary from 15.0 to 20.4 T, the maximum critical field $H_c(\mathbf{m})$ varies from 18.4 to 20.4 T. In the equatorial plane, $H_c^{(n)}(\mathbf{m})$ is a maximum when $\mathbf{m} = \pm \mathbf{y}'_n$, corresponding to azimuthal angles $\psi = -\pi/6 + n\pi/3$ or $5\pi/6 + n\pi/3$. When $H_c^{(n)}(\mathbf{m})$ reaches a maximum value, the critical fields for the other two domains reach their minimum values. Because Le Bras *et al.*[34] restricted consideration to a single magnetic domain, their predicted critical field has a period of $\Delta\psi = \pi$, rather than $\Delta\psi = \pi/3$ as found here.

For $\mathbf{m}$ along a cubic axis such as $\mathbf{z}$, several experimental groups[4,5,18] reported that $H_c = 18.8$ T, which is about 1.4 T lower than our result. To explain this disagreement, we examine the limitations of our variational approach. In equilibrium, the classical energy E_i at each Fe^{3+} site must be a minimum so that the forces $\mathbf{F}_i = \partial E_i/\partial \mathbf{S}_i$ on the spin $\mathbf{S}_i$ vanish. The forces are quite small above H_c, indicating that the variational
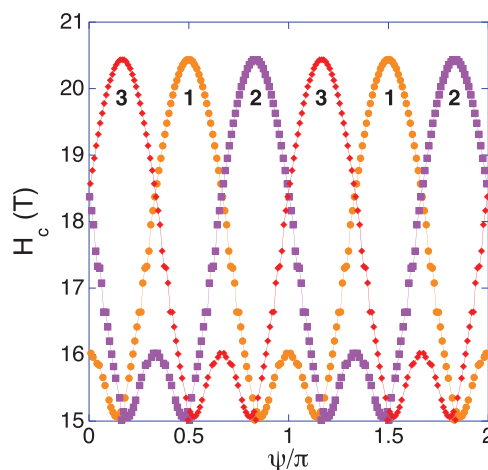

FIG. 3. (Color online) The critical fields for domains 1 (circles), 2 (squares), and 3 (diamonds) vs ψ in the equatorial [1,1,1] plane normal to the polarization.

state provides an excellent description of the AF phase. With increasing field below H_c, the forces grow in magnitude as the variational spin state of the cycloid becomes compromised. Because it provides an upper bound to the cycloidal energy, our variational approach will therefore underestimate rather than overestimate the critical field. Hence, the limitations of this approach cannot explain the overestimation of the critical field for $\mathbf{m} = \mathbf{z}$.

But our classical model does not account for quantum spin fluctuations, which will differently affect the energies of the cycloidal and AF phases. For the geometrically frustrated antiferromagnet $CuCrO_2$, quantum fluctuations suppress the critical field[35] for the transition from a cycloidal to a collinear phase when the easy-axis anisotropy is small. In $BiFeO_3$, quantum fluctuations should also lower the critical field $H_c(\mathbf{m})$ from the classical values provided in this paper. For $S = 5/2$, the $1/(2S + 1)$ effects of quantum fluctuations may possibly suppress the critical field by about 17%.

IV. COMPARISON WITH MEASUREMENTS

The comparison of predictions for $H_c(\mathbf{m})$ with measurements is complicated by two factors. As found in the polarization measurements of Tokunaga *et al.*,[4] hysterisis may be produced by the first-order transition between the cycloidal and AF phases. Due to the competition between magnetic domains, measurements may also yield different results depending on which domain is probed. Perhaps as a consequence, Park *et al.*[5] reported that the jump in the electric polarization can occur at a slightly lower or higher field than the drop in the magnetization. By providing the critical fields for all three domains, our results may help to separate these two complicating factors.

For $\mathbf{m}$ between $\mathbf{z} = (0,0,1)$ and $(1,1,0)$, Tokunaga *et al.*[4] observed that $H_c(\mathbf{m})$ peaks at $\mathbf{z}' = (1,1,1)$ with a value of 24 T. On the other hand, Fig. 4(a) indicates that $H_c(\mathbf{z}') = 22.4$ T when $\theta = \cos^{-1}(\mathbf{z}' \cdot \mathbf{z}) = 0.304\pi$ (54.7°). Notice that domain 1 has the lowest energy and highest critical field for all angles $\theta = \cos^{-1}(\mathbf{m} \cdot \mathbf{z})$ along this longitude. But even a sample with a distribution of magnetic domains 1, 2, and 3 should still exhibit a maximum critical field at $\theta = 0.304\pi$. Tokunaga *et al.* also observed that $H_c(\mathbf{m}) = 18$ T for $\mathbf{m} = (-1,1,0)$, which is a bit smaller than our prediction of 18.4 T. Hence, their measurements yield a net range in H_c of roughly 6 T, which is about 50% larger than predicted in this paper. By contrast, Park *et al.*[5] compared the critical fields for three different orientations $\mathbf{m}$ and found that $H_c(\mathbf{m}) = 19$ T is smallest when $\mathbf{m} = \mathbf{z}'$.

Just as puzzling, Tokunaga *et al.*[4] did not observe the predicted minimum in $H_c(\mathbf{m})$ between $(0,0,1)$ and $(-1,1,0)$ for $\theta = 0.166\pi$ (30°), at the border between domains 1 and 3 in Fig. 4(b). This suggests that their sample is evenly divided between domains 1 and 3 so that the measured critical field is an average of $H_c^{(1)}(\mathbf{m})$ and $H_c^{(3)}(\mathbf{m})$. If that is the case, then the width of the magnetic transition should increase away from $\theta = 0.166\pi$. It may still be possible to observe the predicted minimum by applying and then removing a field far above $H_c(\mathbf{m})$ prior to each measurement. In Fig. 4(b), the critical field for domain 1 is terminated at about 15.3 T, below which the AF phase is not stable and $H_c^{(3)}(\mathbf{m})$ is not defined.
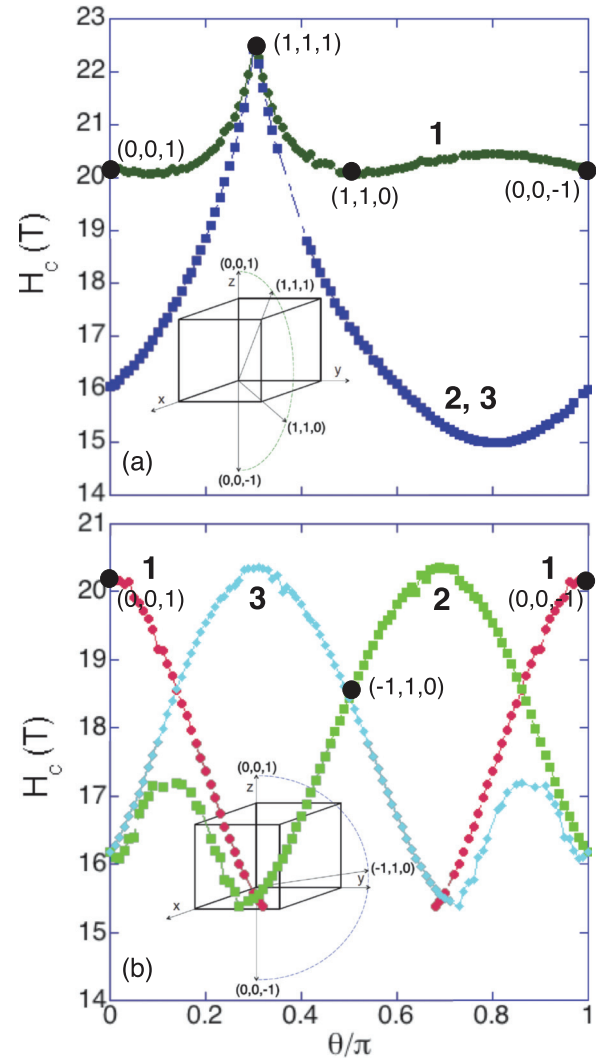

FIG. 4. (Color online) The critical field for two longitudes connecting $\mathbf{z} = (0,0,1)$ with $(0,0,-1)$ through either (a) $(1,1,0)$ or (b) $(-1,1,0)$ with $\theta = \cos^{-1}(\mathbf{m} \cdot \mathbf{z})$. The insets show the two trajectories for the cubic unit cell.

V. CONCLUSION

To conclude, we have shown that the competition between magnetic domains produces a complex dependence of the critical field $H_c(\mathbf{m})$ on orientation $\mathbf{m}$. In some cases, measurements of the critical field may average over the susceptibility or polarization of more than one magnetic domain. We hope that this work will inspire more comprehensive measurements of the orientation dependence of $H_c(\mathbf{m})$ for this highly important material.

[1] J. R. Teague, R. Gerson, and W. J. James, Solid State Commun. **8**, 1073 (1970).

[2] I. Sosnowska, T. Peterlin-Neumaier, and E. Steichele, J. Phys. C **15**, 4835 (1982).

[3] Y. F. Popov, A. K. Zvezdin, G. P. Vorob'ev, A. M. Kadomtseva, V. A. Murashev, and D. N. Rakov, JETP Lett. **57**, 69 (1993).

[4] M. Tokunaga, M. Azuma, and Y. Shimakawa, J. Phys. Soc. Jpn. **79**, 064713 (2010).

[5] J. Park, S.-H. Lee, S. Lee, F. Gozzo, H. Kimura, Y. Noda, Y. J. Choi, V. Kiryukhin, S.-W. Cheong, Y. Jo, E. S. Choi, L. Balicas, G. S. Jeon, and J.-G. Park, J. Phys. Soc. Jpn. **80**, 114714 (2011).

[6] D. Lebeugle, D. Colson, A. Forget, M. Viret, A. M. Bataille, and A. Goukasov, Phys. Rev. Lett. **100**, 227602 (2008).

[7] S. Lee, W. M. Ratcliff, II, S.-W. Cheong, and V. Kiryukhin, Appl. Phys. Lett. **92**, 192906 (2008); S. Lee, T. Choi, W. Ratcliff, II, R. Erwin, S.-W. Cheong, and V. Kiryukhin, Phys. Rev. B **78**, 100101(R) (2008).

[8] J. Jeong, E. A. Goremychkin, T. Guidi, K. Nakajima, G. S. Jeon, S.-A. Kim, S. Furukawa, Y. B. Kim, S. Lee, V. Kiryukhin, S.-W. Cheong, and J.-G. Park, Phys. Rev. Lett. **108**, 077202 (2012).

[9] M. Matsuda, R. S. Fishman, T. Hong, C. H. Lee, T. Ushiyama, Y. Yanagisawa, Y. Tomioka, and T. Ito, Phys. Rev. Lett. **109**, 067205 (2012).

[10] Z. Xu, J. Wen, T. Berlijn, P. M. Gehring, C. Stock, M. B. Stone, W. Ku, G. Gu, S. M. Shapiro, R. J. Birgeneau, and G. Xu, Phys. Rev. B **86**, 174419 (2012).

[11] J. M. Moreau, C. Michel, R. Gerson, and W. D. James, J. Phys. Chem. Sol. **32**, 1315 (1971).

[12] M. Ramazanoglu, W. Ratcliff, II, Y. J. Choi, S. Lee, S.-W. Cheong, and V. Kiryukhin, Phys. Rev. B **83**, 174434 (2011).

[13] J. Herrero-Albillos, G. Catalan, J. A. Rodriguez-Velamazan, M. Viret, D. Colson, and J. F. Scott, J. Phys.: Condens. Matter **22**, 256001 (2010).

[14] I. Sosnowska and R. Przenioslo, Phys. Rev. B **84**, 144404 (2011).

[15] R. S. Fishman, N. Furukawa, J. T. Haraldsen, M. Matsuda, and S. Miyahara, Phys. Rev. B **86**, 220402(R) (2012).

[16] M. Cazayous, Y. Gallais, A. Sacuto, R. de Sousa, D. Lebeugle, and D. Colson, Phys. Rev. Lett. **101**, 037601 (2008).

[17] D. Talbayev, S. A. Trugman, S. Lee, H. T. Yi, S.-W. Cheong, and A. J. Taylor, Phys. Rev. B **83**, 094403 (2011).

[18] U. Nagel, R. S. Fishman, T. Katuwal, H. Engelkamp, D. Talbayev, H. T. Yi, S.-W. Cheong, and T. Rõõm, Phys. Rev. Lett. **110**, 257201 (2013).

[19] R. S. Fishman, Phys. Rev. B **87**, 224419 (2013).

[20] R. S. Fishman, J. T. Haraldsen, N. Furukawa, and S. Miyahara, Phys. Rev. B **87**, 134416 (2013).

[21] A. M. Kadomtseva, A. K. Zvezdin, Yu. F. Popv, A. P. Pyatakov, and G. P. Vorob'ev, JTEP Lett. **79**, 571 (2004).

[22] C. Ederer and N. A. Spaldin, Phys. Rev. B **71**, 060401(R) (2005).

[23] A. P. Pyatakov and A. K. Zvezdin, Eur. Phys. J. B **71**, 419 (2009).

[24] K. Ohoyama, S. Lee, S. Yoshii, Y. Narumi, T. Morioka, H. Nojiri, G. S. Jeon, S.-W. Cheong, and J.-G. Park, J. Phys. Soc. Jpn. **80**, 125001 (2011).

[25] P. Chen, Ö. Günaydın-Sen, W. J. Ren, Z. Qin, T. V. Brinzari, S. McGill, S.-W. Cheong, and J. L. Musfeldt, Phys. Rev. B **86**, 014407 (2012).

[26] F. Bai, J. Wang, M. Wuttig, J. F. Li, N. Wang, A. P. Pyatakov, A. K. Zvezdin, L. E. Cross, and D. Viehland, Appl. Phys. Lett. **86**, 032511 (2005).

[27] R. deSousa, M. Allen, and M. Cazayous, Phys. Rev. Lett. **110**, 267202 (2013).

[28] M. Ramazanoglu, M. Laver, W. Ratcliff, II, S. M. Watson, W. C. Chen, A. Jackson, K. Kothapalli, S. Lee, S.-W. Cheong, and V. Kiryukhin, Phys. Rev. Lett. **107**, 207206 (2011).

[29] I. Sosnowska and A. K. Zvezdin, J. Mag. Mag. Matter. **140–144**, 167 (1995).

[30] H. Katsura, N. Nagaosa, and A. V. Balatsky, Phys. Rev. Lett. **95**, 057205 (2005).

[31] M. Mostovoy, Phys. Rev. Lett. **96**, 067601 (2006).

[32] I. A. Sergienko and E. Dagotto, Phys. Rev. B **73**, 094434 (2006).

[33] D. Lebeugle, D. Colslon, A. Forget, and M. Viret, Appl. Phys. Lett. **91**, 022907 (2007).

[34] G. Le Bras, D. Colson, A. Forget, N. Genand-Riondet, R. Tourbot, and P. Bonville, Phys. Rev. B **80**, 134417 (2009).

[35] R. S. Fishman, Phys. Rev. B **84**, 052405 (2011).